Atmos. Meas. Tech. Discuss.,
doi:10.5194/amt-2017-191-RC1, 2017

Atmospheric Measurement Techniques Discussions

Interactive comment on "Variability of the Brunt-Väisälä frequency at the OH*-layer height" *by* Sabine Wüst et al.

C. von Savigny (Referee)

csavigny@physik.uni-greifswald.de

Received and published: 20 July 2017

Dear Christian,

Thank you very much for your valuable comments. I tried to include them as best as possible.

One thing I realized during the revision of the manuscript: On page 3, line 30 (original manuscript), I wrote "Error propagation shows that an error of 10% in the BV frequency leads to an error of 20% in the density of wave potential energy (see Wüst et al., 2016)." This mentioned calculation was included in the first version of Wüst et al. (2016). Due to re-arrangements of the manuscript in the review process, I deleted

Printer-friendly version

Discussion paper

it. Therefore, I now included the calculation in this manuscript and deleted the reference to Wüst et al. (2016).

General comments:

This is a generally well written study on the variability of the Brunt-Väisälä (BV) frequency in the MLT region. Knowledge of the BV frequency is relevant for the derivation of gravity wave related parameters, e.g. from ground-based observations of MLT temperature fluctuations. The results presented are useful for the aeronomy community and particularly for the groups operating ground-based OH rotational temperature spectrometers. I have no major objections against the publication of this manuscript, but ask the authors to consider the specific comments listed below.

Specific comments:

- Page 1, line 16: "which are“ -> "which is“ Done
- Page 2, line 25: “The same holds for the BV frequency” It’s not clear, what “The same” refers to. Please rephrase. Done
- Page 3, line 25: I suggest mentioning the factor 2 pi in the context of BV period and BV frequency. I think the formula/values are not entirely consistent. Often the factor 2 pi is already included in the definition of the BV frequency. It should be clear, whether “frequency” refers to “angular frequency” or not.

  I inserted the following sentences after formula (3) “This formula refers to the angular BV frequency. Even if not explicitly mentioned in the following, the terms BV frequency or BV period always denote the angular values.” Furthermore, I included $2\pi/N$ after BV period (former page 3, line 25).

- Page 6, equation (4): I’m not sure the normalization by the norm of vector f is correct. One should divide by the sum of all elements of vector f, right? The

norm, however, has a very different value, i.e. the square root of the summed up squared vector elements - at least according to the standard definition.

You are right, the calculation is correct but the formula is wrong. I corrected it.

This probably only affects equation (4) and not the actual calculation of the OH* equivalent BV frequencies?

- Page 6, line 5: Regarding the OH* layer height: If I understand correctly, the layer height is simply the height grid point with the maximum VER, right?
Yes, that's true

It would be better to use centroid altitude, i.e. altitude weighted with the VER profile. If the altitude with maximum VER is used, the altitudes will be affected by the vertical sampling of the SABER limb measurements and by the retrieval altitude grid. I assume, the effects will be very small, though, but it would be good to motivate, why the height of the VER maximum is used here.

I analysed the first half of the year 2004. This year was arbitrarily chosen. The mean difference between the centroid altitude and the peak altitude is ca. 0.7 km, the skewness of the VER-distribution is 0.8 which is not a very large value.

Since the vertical resolution of the SABER data is ca. 300–400 m, a difference of 0.7 km corresponds to 2 data points at maximum. Taking into account the FWHM of 7–8 km of the OH*-layer and the calculation method of the climatology of the Brunt-Väisälä frequency (least squares fit to the daily mean values of the Brunt-Väisälä frequency), I would judge the effect as negligible.

I inserted in the manuscript: "The assumption of a Gaussian-shaped OH*-layer is certainly simplified. In most cases, the OH*-layer follows a slightly asymmetric form with a positive skewness. That means the centroid height is a little bit higher (for example, ca. 0.7 km averaged over the first half of the

year 2004) than the height of the maximum VER. Due to these small differences and the averaging which is applied afterwards to the Gaussian-weighted squared BV frequency, this simplified approach can be justified."

Also: the OH VER profile is not Gaussian. Assuming a Gaussian will also affect the results somewhat. I think you should at least mention that the actual VER profile is not Gaussian.

See above.

- Page 9, line 11: "For ENVISAT [..] on board of SCIAMACHY" –> "For SCIAMACHY [..] on board of Envisat" SCIAMACHY is the instrument, Envisat the satellite. Done.
- Page 9, line 15: Regarding the agreement between SCIA and SABER OH emission altitudes:

  Centroid altitude and altitude of maximum VER may be quite different (up to 2 km, I reckon), because the OH VER profile is asymmetric. Centroid altitude will be systematically larger than the VER-max altitude

  Remaining tidal effects between the average SABER local time and the SCIA local time (between 21 and 22 at 40 – 50 N) may also contribute to differences

  The vertical shifts between the different Meinel-bands may also play a role So, considering these differences, the agreement is quite good.

  Thank you for this hint. I mentioned it in the manuscript "In contrast to our analysis, von Savigny (2015) refers to the centroid altitude, while we show the altitude of maximum VER. These values differ, if the OH VER profile is asymmetric. Furthermore, remaining tidal effects due to different overpass times of both satellites and vertical shifts between the different Meinel-bands may also play a role. So, considering these possible sources of inconsistencies, the agreement is even quite good."

- Page 9, line 25/26: The linear trend in OH height is interesting and fairly consistent with a trend determined in our recent paper (Teiser & von Savigny, Variability of OH(3-1) and OH(6-2) emission altitude and volume emission rate from 2003 to 2011, JASTP, 161, 28-42, 2017). In this study, the trend in OH(3-1) centroid altitude (averaged between 5S and 30N) is about -20 m/yr. Higher northern latitudes are not covered, unfortunately. And one has to be careful, because trends in the SCIAMACHY limb pointing data may also play a role at this level. It is, however, interesting to note the qualitative and quantitative agreement between the different results.

  Indeed, that's interesting and I included it therefore in the manuscript p. 12, ll.6–8 (version with changes marked).

- References: The list of references contains several inconsistencies and typos, i.e.: spacing between initials is not consistent, e.g., "R. A." vs. "C.J."; in several cases the hyphen is missing between "Sol." and "Terr." for JASTP papers; in some cases there are periods between paper title and journal name, rather than commas.

  Page 12, line 23: delete extra space in "T. ," Done.

  Page 14, line 19: delete extra space in "OH (3-1)" Done.

  Page 14, line 2 bottom-up: delete extra space in "O (1S)" Done.

  Page 14, last line: comma after paper title missing. Done.

  I checked the whole reference list for inconsistencies and hope that I could identify all.

Printer-friendly version

Discussion paper

Atmos. Meas. Tech. Discuss.,
doi:10.5194/amt-2017-191-RC2, 2017

Atmospheric Measurement Techniques Discussions

Interactive comment on "Variability of the Brunt-Väisälä frequency at the OH*-layer height" *by* Sabine Wüst et al.

Anonymous Referee #2

Received and published: 24 July 2017

Thank you very much for your valuable comments. I tried to include them as best as possible.
One thing I realized during the revision of the manuscript: On page 3, line 30 (original manuscript), I wrote "Error propagation shows that an error of 10% in the BV frequency leads to an error of 20% in the density of wave potential energy (see Wüst et al., 2016)." This mentioned calculation was included in the first version of Wüst et al. (2016). Due to re-arrangements of the manuscript in the review process, I deleted it. Therefore, I now included the calculation in this manuscript and deleted the reference to Wüst et al. (2016).

Printer-friendly version

Discussion paper

The authors describe a method of calculating a value for the Brunt-Väisälä (BV) frequency, that can be used at the altitude of OH* emissions near the mesopause (denoted OH*-equivalent BV frequency), based on temperature and volume emission rate (VER) profiles from the SABER instrument on the TIMED satellite.

They use 14 years of SABER profiles (2002-2015) in the vicinity of the Alpine region (43.93–48.09°N and 5.71–12.95°E) to obtain a climatology of the BV frequency in that region. They demonstrate that the BV frequency has an annual pattern which is repeated from year to year, even though there are considerable differences between individual years, with the largest variability occurring in the winter season. The climatology is specified in terms of an annual, semi-annual and ter-annual oscillations which account for 74% of the variation observed. Almost 98% of all of the nightly averaged OH*-equivalent BV frequencies fall within the range of the climatology +/-10%.

The authors propose to use this climatology together with measurements of gravity waves obtained from a network of GRIPS-type (Ground-based Infrared P-branch Spectrometers) instruments already deployed in the Alpine region to enable them to estimate values of the nightly averaged density of potential energy (per unit mass) for the gravity waves detected. In an earlier publication, the authors reported that a 10% uncertainty in the BV frequency gives rise to a 20% uncertainty in the density of wave potential energy.

The manuscript is well organised and the intention of the authors is clear in almost all instances (however, see some of the specific comments below). The methods used to calculate the OH*-equivalent BV climatology are valid (see specific point relating to equation 4 on page 6) . The approach outlined could be employed by other ground-based observers, and it is therefore a valuable contribution to this field of study. The work is suitable for publication in AMT, provided that the specific points below are addressed.

Specific comments

Page 1, line 14; rephrase 'the derivation of . . . Brunt-Väisälä frequency provided.' as 'the derivation of the density of gravity wave potential energy, provided that the Brunt-Väisälä frequency is known.' Done

Page 2, line 3; replace 'like for example' by 'such as'. Done

Page 2, line 8; g is the acceleration due to gravity, not the gravitational constant. Done

Page 2, line 17; omit the word 'etc'. Done

Page 2, line 20; the meaning of the phrase '. . . nor the relation of potential and kinetic energy.' Is not clear. Please reword the entire sentence. Done

Page 3, line 1; {uppercase greek gamma} (more usually written with a subscript-d) when referring to the dry adiabatic lapse rate) is defined as (gamma subscript-d = -dT/dz). I additionally provided this information to avoid confusion.

Therefore the minus sign should be omitted and the phrase 'a value of' inserted before the numerical value. I wrote "where Γ_d is the dry-adiabatic lapse rate defined as the vertical adiabatic temperature decrease with a value of 9.8 K/km."

Page 3, line 4; suggest 'the direct calculation of' instead of 'to directly calculate'. Done

Page 3, line 9; suggest 'do not provide temperature . . . ' instead of 'not even temperature . . .'. Done

Page 3, lines 12-15; this sentence is unwieldy. It should be separated into two sentences. The first sentence should end after 'the BV frequency' on line 13. The second sentence might be rephrased along the lines: 'While the latter might be of

Printer-friendly version

Discussion paper

higher accuracy in most cases, lack of coincidence in either time or space of the complementary measurement with the passage of a wave could result in unrepresentative BV values'. Done

Page 3, line 24;insert a comma after '(40°N, 88°W)'. Done

Page 3, line 26; for clarity use '2.12×10-2 s-1' instead of '2.12Âů10-2 s-1' and use '(∼

4.9 min)' instead of '(= 4.9 min)' on line 27. Done, also for 2.29×10^{-2} in the same line. "≈" also inserted in the lines above.

Page 4, line 12; replace 'denoted with' by 'denoted as'. Done

Page 5, line 6; omit the word 'well' before 'suitable'. Done

Page 5, lines 9/10; suggest rewording the sentence as follows: 'An overview of the large number of SABER publications is available at http://saber.gats-inc.com/publications.php.' Done

Page 5, line 12; '15 μm' instead of '15 um'. Done

Page 6, line 8; why does equation 4 contain 1/|f| instead of 1/(sum over i of fi) ?. Corrected, the calculation is right, the formula was wrong.

Page 6, line 12; rephrase as 'This was also the approach presented and discussed in Wüst et al. (2016) and Wüst et al. (2017).'. Done

Page 6, line 16; replace 'unproportionally' by 'disproportionally'. Done

Page 6, line 24; replace 'whereas' by 'although'. Done

Page 7, line 6; '0.023 s-1' would seem to be more accurate than '0.0235 s-1' for the OH*-equivalent BV value. Ok

Page 7, lines 14/15; suggest 'and maxima at 9 km, 8 km and 8 km approximately for DOY 40 (February), 110 (April), and 285 (October) respectively (thick line in fig. 2 (b)).' instead of 'and three maxima . . . and 285 (October, thick line in fig. 2 (b)).'.

Done

Page 7, line 21; replace ‘mid’ by ‘middle’. Done

Page 7, line 22; replace ‘motivates’ by ‘suggests’ and omit ‘a’ before ‘harmonic’. Done

Page 7, line 33; suggest replace the final two sentences by ‘This 60-day oscillation is probably not a geophysical period but the may result instead from the local time sampling of the satellite or the fact that it performs a yaw maneuver once every 60 days (rotating through 180 degrees) to keep SABER viewing away from the sun.’. Done but left out “the” before “may result”.

Page 8, line 2; The meaning of the sentence beginning ‘Depending on the accuracy needed . . . ‘ is not clear. Please rephrase to clarify the intended point . Sentence changed accordingly.

Page 8, line 6; please be consistent in the use of ‘DoY’ or ‘DOY’ (lines 12-16 on page 7). Done, changed to DoY everywhere in the document.

Page 8, line 16; replace ‘which influences also {uppercase greek gamma}.’ by ‘which also influences {uppercase greek gamma}.’. Done

Page 8, lines 16-18; the sentence beginning ‘According to Wüst et al. (2017) . . .’ is confusing. It appears to confuse the variation of g and {uppercase greek gamma} with altitude, and the effect of both of these on N-squared. The value and unit quoted on line 18 (9.81 K/km) as stated refer to g, but it is actually the unit of {uppercase greek gamma}. Please correct this sentence. Done

Page 8, lines 24-25; suggest ‘This behaviour has been reported previously by Bills and Gardner (1993) and Wüst et al. (2016).’ instead of the sentence ‘This behaviour . . . for example.’ Done

Page 8, line 27; suggest ‘In contrast to the approach presented here . . . ’ instead of ‘Different to the approach presented here . . . ’. Done

Page 9, line 1; suggest ‘Nevertheless, the SABER-based OH*-equivalent BV frequency is systematically higher than the one based on CIRA (0.019–0.022 1/s) regardless of the calculation method employed here or in Wüst et al. (2016).’ instead of ‘Independent of these facts, . . . CIRA (0.019–0.022 1/s)’ Done

Page 9, line 2; Please be consistent in the typography of units used for BV values (1/s) used here and also on page 17 and page 18 (y-axis label) or (s-1) used on pages 3, 7 and 10. Changed to s-1.

Page 9, line 4; replace ‘and in parts also’ by ‘in some instances’; replace ‘on case study base’ by ‘on a case study basis’. Done

Page 9, line 6; suggest replace ‘base’ by ‘basis’. Done

Page 9, lines9-10; the emission altitude presented in Figure 2(a) is not the mean OH(3-1) emission altitude but is instead the emission altitude of the SABER OH- B channel as described on page 5 (lines 21-26). Figure 2(a) for the period September to March suggests that the mean emission altitude range is 85-87 km, not 86.0–86.5 km as stated. This comment presumably refers to lines 14–15. The formulation I used was misleading, I am sorry for that. I changed the sentences now to “For these months and the addressed latitudinal range (43.93–48.09°N), the emission altitude of the SABER OH-B channel presented in our fig. 2 (a) (thick line) reaches 84.5-87.5 km and shows reasonable agreement with a mean value of ca. 86 km.”

Page 9, lines 26 and 30; please use ‘km/year’ as the unit instead of ‘km/a’. Done

Page 10, line 5; use ‘2.35×10-2 s-1’ instead of ‘2.35Âu˚ 10-2 s-1’ and suggest

‘during 2002-2015’ instead of ‘during 14 years’. Done

Page 10, line 8; consider inserting the word ‘mean’ before ‘OH*-‘. Done

Page 10, line 11; consider inserting the word ‘mean’ before ‘curve‘. Done

Page 12, lines 32-33 and page 13, lines 1-2; these references are not in alphabetical order of surname. Done

Page 15, Table 1; Why not use column headings ”annual”, “semi- annual” and “ter-annual” (using quotation marks around each heading to indicate that they are approximate periods) instead of ‘1st oscillation 2nd oscillation 3rd oscillation’?

Figure 3 on page 20 uses ‘annual, semi-, and ter-annual’ to describe these oscillations. Changed

Page 15, lines 4-5; use ‘2.32×10-2 s-1’ instead of ‘2.32Âu˚ 10-2 s-1’ Done

Page 17, caption of Figure 1; omit ‘a’ in ‘. . . but show a comparatively . . ..’. Done

Pages 18/19/20, label on x-axis is written as ‘DoY’, whereas it is written as ‘DOY’ on page 7 (lines12 – 16) and page 8 (line 6) as ‘DoY’. Please be consistent in this label. Changed DOY to DoY in the whole manuscript

Page 21, caption of Figure 4, final sentence; suggest ‘The temperature values are offset by +30 K per month for all months except January.’. Done

Variability of the Brunt-Väisälä frequency at the OH*-layer height

Sabine Wüst [1], Michael Bittner [1, 2], Jeng-Hwa Yee [3] , Martin G. Mlynczak [4], James M. Russell III [5]

[1] Deutsches Fernerkundungsdatenzentrum, Deutsches Zentrum für Luft- und Raumfahrt, 82234 Oberpfaffenhofen, Germany
[2] Institut für Physik, Universität Augsburg, 86159 Augsburg, Germany
[3] Applied Physics Laboratory, The Johns Hopkins University, Laurel, Maryland, USA
[4] NASA Langley Research Center, Hampton, USA
[5] Center for Atmospheric Sciences, Hampton, USA
Correspondence to: Sabine Wüst (sabine.wuest@dlr.de)

Abstract. In and near the Alpine region, the most dense sub-network of identical NDMC instruments (Network for the Detection of Mesospheric Change, http://wdc.dlr.de/ndmc) can be found: five stations are equipped with OH*-spectrometers which deliver a time series of mesopause temperature each cloudless or only partially cloudy night. These measurements are suitable for the derivation of the density of gravity wave potential energy, provided that the Brunt-Väisälä frequency is known~~,the derivation of the density of gravity wave potential energy – knowledge about the Brunt-Väisälä frequency provided.~~

However, OH*-spectrometers do not deliver vertically-resolved temperature information, which ~~are~~ is necessary for the calculation of the Brunt-Väisälä frequency. Co-located measurements or climatological values are needed.

We use 14 years of satellite-based temperature data (TIMED-SABER, 2002–2015) to investigate the inter- and intra-annual variability of the Brunt-Väisälä frequency at the OH*-layer height between 43.93–48.09°N and 5.71–12.95°E and provide a climatology.

1 Introduction

The Brunt-Väisälä frequency (BV frequency) is an important parameter in gravity wave theory. It is not only the highest possible frequency for gravity waves, it is also necessary when calculating different gravity wave parameters ~~like for example~~such as the density of wave potential energy averaged over a specific time period (see e.g. Wüst et al., 2016)

$$E_{pot}\left(\overline{T'^2}, T, \frac{dT}{dz}\right) = \frac{1}{2}\frac{g^2\overline{T'^2}}{N^2} \quad (1)$$

where

N is the BV frequency,

g the acceleration due to gravity~~gravitational constant~~,

T the temperature, and

$\overline{T'^2}$ the mean squared normalized temperature fluctuation, i.e., the mean squared temperature fluctuation relative to the background temperature. It is calculated as follows:

$$\overline{T'^2} = \frac{1}{n}\sum_{i=1}^{n} {T'_i}^2 \quad (2)$$

with the normalized temperature fluctuation T'_i at time step i of n time steps in total.

Energy and momentum are transported by gravity waves over large distances. Through interactions with other dynamical processes in the atmosphere (such as planetary waves, tides, other gravity waves ~~etc.~~) they can strongly influence atmospheric dynamics and are therefore regarded as an essential mechanism within atmospheric layer coupling. Case studies (e.g. Lu et al., 2015; Lu et al., 2009) based on LIDAR data (in the strato- and mesosphere) show that ~~neither~~ the amount of potential energy is not constant with height and that ~~nor~~ the relation of potential and kinetic energy also varies height-dependently. Tsuda et al. (2000), for example, report that kinetic energy density dominates potential energy density (per unit mass) by a factor of 5/3 to 2 in the stratosphere based on GPS radio occultation data. Placke et al. (2013) use LIDAR data and show a minor deviation at mesopause heights from the value of 5/3 which is expected following linear gravity wave theory.

Also ~~The same holds for~~ the BV frequency~~: it~~ is not constant with height since it varies with the temperature and its vertical gradient as the following formula shows (e.g. Andrews, 2000):

$$\mathrm{N}\left(T, \frac{dT}{dz}\right) = \sqrt{\frac{\mathrm{g}}{\mathrm{T}}\left(\frac{\mathrm{dT}}{\mathrm{dz}} - \Gamma\Gamma_d\right)} \quad (3)$$

where Γ_dΓ is the dry-adiabatic lapse rate defined as the vertical adiabatic temperature decrease with a value of -9.8 K/km. This formula refers to the angular BV frequency. Even if not explicitly mentioned in the following, the terms BV frequency or BV period always denote the angular values.

Many measurement techniques suitable for the investigation of gravity waves provide vertical temperature profiles; this allows to directly calculate the direct calculation of the BV frequency and the density of wave potential energy (see e.g. Kramer et al., 2015; Mzé et al., 2014; Rauthe et al., 2008 to mention just a few). For OH* observation techniques, the situation is different: OH* spectrometers deliver information about temperature, also horizontally-resolved—if operated in a scanning mode (see e.g. Wachter et al., 2015)—but vertically averaged over the OH*-layer. OH* imaging systems provide brightness maps (e.g. Sedlak et al. (2016) and Hannawald et al. (2016) who address a small part of the sky and Garcia et al. (1997) who operate an all-sky system), they do not but not even provide temperature information for the majority of instruments. This is only possible when using narrow-band filters (see Pautet et al., 2014).

In order to deduce the density of wave potential energy from OH* spectrometer measurements, one needs to rely on temperature climatologies or complementary measurements for the derivation of the BV frequency. While the latter might be of higher accuracy in most cases, lack of coincidence in either time or space of the complementary measurement with the passage of a wave could result in unrepresentative BV values whereas the latter might be of higher accuracy in most cases – a sufficiently low mistime and misdistance provided (see Wendt et al., 2013 for the quantification of typical temperature differences due to mistime and misdistance).

In our preceding publication Wüst et al. (2016), we used TIMED-SABER (Thermosphere Ionosphere Mesosphere Energetics Dynamics, Sounding of the Atmosphere using Broadband Emission Radiometry) measurements for this purpose with the focus on three mid-European and one northern-European NDMC-station (Network for the Detection of Mesospheric Change, http://wdc.dlr.de/ndmc). The BV (angular) frequency derived for the OH*-layer height for the mid-latitude station Haute-Provence (43.93°N, 5.71°E, OHP), France is 0.022 s^{-1} (yearly average) with a standard deviation of 0.002 s^{-1} showing a minimum in winter and a maximum in summer. With a yearly mean of 0.021 s^{-1} and the same standard deviation as for OHP, it is slightly lower for the high-latitude station ALOMAR (69.28°N, 16.01°E), Norway. For measurements at the Urbana Atmospheric Observatory (40°N, 88°W), United States of America, over a 6-month period from January through June 1991, Bills and Gardner (1993) report a BV period $2\pi/N$ near 90 km height of 5.2 min (≈= 0.020 s^{-1}) during the winter months and 4.3 min (≈= 0.024 s^{-1}) during spring and early summer. She et al. (1991) compute a BV frequency of

2.12 × 10^{-2} s^{-1} (≙ 4.9 min) and 2.29 × 10^{-2} s^{-1} (≙ 4.6 min) averaged between 86 km and 100 km for two nightly measurements in 1990 at Fort Collins (40.6°N, 105°W), United States of America.

Error propagation shows that an error of 10% in the BV frequency leads to an error of 20% in the density of wave potential energy E_{pot} (see Wüst et al., 2016):

$$\pm\left|\frac{\partial E_{pot}}{\partial N}\Delta N\right| \overset{(1)}{=} \pm\left|-2\cdot\frac{g^2\overline{T'^2}}{N^3}\cdot\Delta N\right| = \pm\left|\frac{g^2\overline{T'^2}}{N^2}\cdot 2\frac{\Delta N}{N}\right| = \pm\left|E_{pot}\cdot 2\frac{\Delta N}{N}\right| \quad (4)$$

Formatiert: Links, Einzug: Hängend: 1,25 cm

Since at least to our knowledge a temperature sounding satellite addressing the mesosphere is not planned for the time after TIMED-SABER and in-situ measurements are rare and not available at every NDMC station, a climatology of the BV frequency is therefore very valuable for our purposes. Of course, gravity waves themselves influence the BV frequency, too. However, due to the thickness of the OH*-layer, small-scale variations cancel out (see e.g. Wüst et al., 2016). Furthermore, we plan to use this climatology for the calculation of the nightly-averaged gravity wave potential energy density based on NDMC measurements. So, the spatial averaging is accompanied by a temporal one which motivates the use of a climatology in this case.

In the Alps and the vicinity of the Alps, there are five NDMC-stations: Oberpfaffenhofen (48.09°N, 11.28°E), the observatory Hohenpeißenberg (47.8°N, 11.0°E), the Environmental Research Station Schneefernerhaus (47.42°N, 10.98°E), Germany, and the observatories Haute Provence (43.93°N, 5.71°E), France, and Sonnblick (47.05°N, 12.95°E), Austria. This is the most dense sub-network of NDMC stations. Therefore, we use vertical SABER profiles of the OH volume emission rate (VER, see section 2) in order to retrieve height and full width at half maximum (FWHM) of the OH*-layer for this geographical region. This information is necessary to calculate the BV frequency weighted for the OH*-layer (in the following denoted with as OH*-equivalent BV frequency) based on vertical temperature profiles of SABER (section 3). We describe seasonal variations of the three parameters, height and FWHM of the OH*-layer as well as OH*-equivalent BV frequency, discuss the results and provide a climatology of the yearly course of the OH*-equivalent BV frequency (section 4).

2 Data and analysis

2.1 Data

The TIMED satellite was launched on 7 December 2001 and the on-board limb-sounder SABER soon started to deliver vertical profiles of kinetic temperature on a routine base from approximately 10 km to more than 100 km altitude with a vertical resolution of about 2 km (Mertens et al., 2004; Mlynczak, 1997). The high vertical resolution is ~~well~~ suitable for the investigation of gravity wave activity. About 1200 temperature profiles are available per day. The latitudinal coverage on a given day extends from about 52° latitude in one hemisphere to 83° in the other (Russell et al., 1999). Due to 180° yaw maneuvers of the TIMED satellite this viewing geometry alternates once every 60 days (Russell et al., 1999). An overview of the large number of SABER publications is available at http://saber.gats-inc.com/publications.php.~~A large amount of SABER publications is available, an overview is given on http://saber.gats-inc.com/publications.php.~~

SABER temperatures are determined from measurements of infrared emission from carbon dioxide in the 15-~~u~~μm spectral interval. A comprehensive forward radiance model incorporating dozens of vibration-rotation bands of CO_2, including isotopic and hot bands, and solving the full set of coupled radiative transfer equations under non-LTE, is the basis for the SABER temperature retrievals. One of the main challenges in estimating kinetic temperature values from the CO_2 brightness temperatures in the mesosphere and upper levels is certainly non-LTE conditions (NLTE), i.e., conditions that depart from local thermodynamic equilibrium. NLTE algorithms for kinetic temperature were employed in the SABER temperature retrieval from version 1.03 on (Lopez-Puertas et al., 2004; Mertens et al., 2004, 2008). Comparisons with reference data sets generally confirm good quality of SABER temperatures (Remsberg et al., 2008).

We use TIMED-SABER temperature and OH-B channel data (volume emission rates, VER) in its latest version (2.0) for the years 2002 to 2015. It was downloaded from the SABER homepage (saber.gats-inc.com). The OH-B channel covers the wavelength range from 1.56 to 1.72 µm, which includes mostly the OH (4-2) and OH (5-3) vibrational transition bands. The mean height difference of the OH (4-2)- and OH (3-1)-emission, which is addressed by the OH*-spectrometers at the Alpine NDMC stations mentioned above, is approximately 500 m (von Savigny et al., 2012) and therefore negligible compared to the FWHM.

According to Noll et al. (2016) and references therein, the total uncertainties for single temperature profiles are about 5 K at 90 km height including systematic uncertainties of ca. 3 K.

As mentioned above, we focus on NDMC stations in or near the Alps. Therefore, we use TIMED-SABER data between 43.93–48.09°N and 5.71–12.95°E. Since the OH*-spectrometers allow only measurements during night, we additionally require SABER measurements between 17 UTC and 5 UTC.

Formatiert: Block, Zeilenabstand: 1,5 Zeilen

2.2 Analysis

The squared BV frequency ${N^2}_i$ is calculated for each SABER height level i between 70 and 100 km altitude where m height levels exist in this height range. Information about the OH*-layer is determined from TIMED-SABER OH-VER profiles. We obtain the maximum VER (in the following denoted as OH*-layer height) and the FWHM from the SABER data file which are then used for the calculation of the Gaussian-weighted squared BV frequency $\overline{N^2\left(T,\frac{dT}{dz}\right)}$. The assumption of a Gaussian-shaped OH*-layer is certainly simplified. In most cases, the OH*-layer follows a slightly asymmetric form with a positive skewness. That means the centroid height is a little bit higher (for example, ca. 0.7 km averaged over the first half of the year 2004) than the height of the maximum VER. Due to these small differences and the averaging which is applied afterwards to the Gaussian-weighted squared BV frequency, this simplified approach can be justified.

In the following, the Gaussian-weighted squared BV frequency ~~latter~~ is referred to as squared OH*-equivalent BV frequency

$$\overline{N^2\left(T,\frac{dT}{dz}\right)} = \frac{1}{\sum_{i=1}^{m-1} f_i \Delta\vec{f}} \sum_{i=1}^{m-1} f_i \cdot \underbrace{\frac{2\cdot g}{T_i+T_{i+1}}\left(\left(\frac{\Delta T}{\Delta z}\right)_i - \Gamma\right)}_{\widehat{N^2}_i} \quad (45)$$

where $\vec{f}$ is the vector of Gaussian weights for a mean equal to the maximum VER and a standard deviation σ as it is related to the FWHM by

$$\mathrm{FWHM} = 2\sqrt{2\ln 2}\,\sigma \approx 2.4\,\sigma \quad (56)$$

This was also the approach presented and discussed in Wüst et al. (2016) and Wüst et al. (2017)~~This approach agrees with the ones presented and discussed in Wüst et al. (2016) and Wüst et al. (2017)~~.

It is also possible to first calculate the Gaussian-weighted temperature and its gradient over the OH*-layer and to use these values afterwards for deriving a squared BV frequency $N^2\left(\bar{T},\frac{\bar{dT}}{dz}\right)$. The latter can be slightly different from $\overline{N^2\left(T,\frac{dT}{dz}\right)}$. Let us for example assume that $\frac{dT}{dz}$ is negative and constant, then height levels of lower temperature have a~~n~~ dis~~un~~proportionally higher BV frequency compared to height levels of higher temperature. Averaging over the whole height range leads to a lower BV frequency compared to the case of averaging temperature and its gradient first and calculating the BV frequency afterwards. Since gravity waves modulate the temperature, they also influence the BV frequency. If one calculates the BV frequency for each height level separately and averages afterwards, as we do, one takes these gravity wave induced fluctuations into account but only according to the OH*-layer height and thickness.

With the selection criteria mentioned above, the number of data sets per year ranges between 509 (for the year 2002) and 590 (for the year 2011) ~~whereas~~ although a matching profile is not available for every day.

3 Results and discussion

The yearly means of the three parameters, OH*-layer height, FWHM, and OH*-equivalent BV frequency, show nearly no variations for the years 2002–2015 (black line in fig. 1 (a)–(c)). They reach ca. 86.5 km and 7.5 km for the OH*-layer height and the FWHM, and 0.023~~5~~ s^{-1} for the OH*-equivalent BV frequency.

However, the yearly means of these parameters are accompanied by varying standard deviations (grey bars in fig. 1 (a)–(c)), which range between approximately 2% for the OH*-layer height, 10% for the OH*-equivalent Brunt-Väisälä frequency, and 20–30% for the FWHM. They are due to characteristic intra-annual variations of the parameters.

The yearly course of the OH*-layer height averaged over the years 2002–2015 varies between ca. 85 km and 87.5 km (thick line in fig. 2 (a)). The minimum is reached for the days of the year (~~DOY~~DoY) 1–10 (January) and 320–366 (November–December), the maximum around ~~DOY~~DoY 90 and 220 (March–April and August). The mean FWHM has a minimum between 6 km and 6.5 km around ~~DOY~~DoY 180, and maxima at 9 km, 8 km and 8 km approximately for DoY 40 (February), 110 (April), and 285 (October) respectively (thick line in fig. 2 (b)).~~three maxima at 9 and 8 km approximately for DOY 40 (February), 110 (April), and 285 (October, thick line in fig. 2 (b)).~~ The mean OH*-equivalent BV frequency ranges between 0.021 s^{-1} for ~~DOY~~DoY 40 (February) and 0.026 s^{-1} for ~~DOY~~DoY 185 (July), approximately (fig. 2 (c), thick line). The coloured lines in fig. 2 (a)–(c) refer to the individual years and show 30-point running means.

So, one can say: the intra-annual variability dominates the inter-annual one by far. This provides the possibility to give an analytic description for the OH*-equivalent BV frequency which is identical for every year. The yearly course of the BV frequency is dominated by a minimum at the beginning of the year and a maximum in the middle of the year looking quite symmetric (see fig. 2 (c)), which ~~motivates~~ suggests the use of a spectral analysis. Therefore, we apply ~~a~~ harmonic analysis (all-step approach) to the daily mean data (diamonds in fig. 3). The harmonic analysis provides amplitude, phase, and period of the oscillations which explain the data variability best (see Bittner et al. (1994) or Wüst and Bittner (2006) for further information about the method). When searching for three oscillations, the annual, semi-annual, and ter-annual mode are found (information about amplitude and phases are given in table 1). The annual mode dominates the other two modes by a factor of 2–3. The semi- and the ter-annual mode are approximately of the same amplitude. The superposition of these three sinusoidals (solid line in fig. 3) explains ca. 74% of the data variability. The data deviate 16% at maximum from this curve; 84.4% and 97.8% of the data are located in a ±5%- and ±10%-interval (dashed lines in fig. 3) around the curve.

The superposition of only two oscillations explains 71% of the data variability. If one searches for four sinusoidals, an additional 60 d-oscillation with an amplitude of $0.02 \cdot 10^{-2}$ s^{-1} is found. This is less than half of the amplitudes of the semi- and the ter-annual modes. This 60-day oscillation is probably not a geophysical period but may result instead from the local

time sampling of the satellite or the fact that it performs a yaw maneuver once every 60 days (rotating through 180°) to keep SABER viewing away from the sun. ~~This 60-day oscillation is probably not a geophysical period but the period of the local time sampling of the satellite. Additionally, the spacecraft does a maneuver and rotates 180 degrees to keep SABER viewing away from the sun.~~ Therefore, we propose to use three sinusoidals with the parameters mentioned in table 1 to approximate the yearly course of the OH*-equivalent BV frequency~~. Depending on the accuracy needed,~~ with an uncertainty interval~~s~~ of ±5% or ±10% to include ca. 84% or 98% of ~~up to 16% can be used~~the data.

As mentioned above, the total uncertainties for single SABER temperature profiles are about 5 K at 90 km height with systematic uncertainties of ca. 3 K. Since we calculate a mean of the OH*-equivalent BV frequency for every D~~o~~oY using data of 14 years and approximate these values by a superposition of harmonic oscillations, we argue that we only have to pay attention to systematic uncertainties. If we assume that the systematic uncertainties change only slightly from one height step to the next one, then they mainly influence the absolute temperature value but not the temperature gradient. Let us assume a "true" temperature $T_1 = 200\ K$ and a measured temperature $T_2 = 203\ K$, then the difference between the "true" squared BV frequency ${N_1}^2$ and the measured one ${N_2}^2$ relative to ${N_1}^2$ is:

$$\frac{{N_1}^2 - {N_2}^2}{{N_1}^2} = \frac{\frac{\mathrm{g}}{T_1}\left(\frac{\mathrm{dT}}{\mathrm{dz}} - \Gamma\right) - \frac{\mathrm{g}}{T_2}\left(\frac{\mathrm{dT}}{\mathrm{dz}} - \Gamma\right)}{\frac{\mathrm{g}}{T_1}\left(\frac{\mathrm{dT}}{\mathrm{dz}} - \Gamma\right)} = \frac{\frac{1}{T_1} - \frac{1}{T_2}}{\frac{1}{T_1}} = \frac{T_2 - T_1}{T_2} \approx 1.5\% \qquad (~~6~~7)$$

For the (non-squared) BV frequency, the difference is ca. 0.75%. That means an uncertainty of ca. 3 K in temperature leads to a relative uncertainty of ca. 1.5% (0.75%) in the (non-)squared BV frequency. This is negligible when using the superposition of the annual, semi-annual, and ter-annual mode with an uncertainty interval of ± 5% or ±10% for the approximation of the OH*-equivalent BV frequency.

A larger effect is caused by the height-dependence of g, which also influences ~~also~~ Γ. According to Wüst et al. (2017), g at mesopause height (in the following denoted with g_{hd}, hd for height-dependent) ~~is~~ still reaches ~~larger~~more than 97% compared to its surface value~~of the literature value (9.81 K/km)~~. Following CIRA-86, the temperature gradient at the mesopause ranges between ca. 1.4 and 2.9 K/km (see figure 4). The straight-forward calculation according to

$$\frac{N^2}{{N_{hd}}^2} = \frac{g}{g_{hd}} \cdot \frac{\frac{dT}{dz} - \frac{g}{c_p}}{\frac{dT}{dz} - \frac{g_{hd}}{c_p}} \qquad (~~7~~8)$$

shows that squared BV frequency ${N_{hd}}^2$is ca. 7% lower compared to the case of constant g.

The dependence of the BV frequency on temperature and its vertical gradient causes the variability during the year. Due to the meridional circulation, the mesopause temperature is high in winter and low in summer. Since the inverse temperature is needed for the calculation of the BV frequency, the latter becomes low in winter and high in summer. This behaviour has been reported previously by Bills and Gardner (1993) and Wüst et al. (2016). ~~This behaviour is reported not only here but also~~

~~in the publication of Bills and Gardner (1993) and Wüst et al. (2016), for example.~~ Figure 5 of Wüst et al. (2016) shows the OH*-equivalent BV frequency for the years 2012/13 above the station OHP based on TIMED-SABER and CIRA data. In contrast to the approach presented here~~Different to the approach presented here~~, the OH*-height and its FWHM are kept constant (86.2 km and 7.9 km calculated for July 2012 to June 2013) there. Nevertheless, the SABER-based OH*-equivalent BV frequency is systematically higher than the one based on CIRA (0.019–0.022 s^{-1}) regardless of the calculation method employed here or in Wüst et al. (2016).~~Independent of these facts, the SABER based OH* equivalent BV frequency is systematically higher than the one based on CIRA (0.019–0.022 1/s).~~

Formatiert: Hochgestellt

The OH*-emission height (and in ~~parts~~ some instances ~~also~~ the FWHM of the OH*-layer) was already investigated on a case study basis~~on case study base~~ about 30–40 years ago mostly relying on rocket-borne or lidar measurements (Good, 1976; von Zahn et al., 1987; Baker and Stair, 1988). The investigation of the OH*-layer on a multi-year data ~~base~~ basis started with the launch of WINDII (Wind Imaging Interferometer) on board of UARS (Upper Atmosphere Research Satellite) in September 1991. Due to the latitudinal range of 42° in one hemisphere to 72° in the other alternating every 36 days (e.g. Shepherd et al., 2006), publications using this data set like for example Zhang and Shepherd (1999) focus on the tropics and low mid-latitudes, and are thus not suitable for a comparison with our results.

For SCIAMACHY (SCanning Imaging Absorption spectroMeter for Atmospheric CHartographY)~~ENVISAT (ENVironmental SATellite)~~ on board of ENVISAT (ENVironmental SATellite)~~ SCIAMACHY (SCanning Imaging Absorption spectroMeter for Atmospheric CHartographY)~~, von Savigny (2015) published a mean OH (3-1) emission altitude for 40–50°N of 85.9 km (January 2003–December 2011, see his table 3). Due to the latitudinal coverage of SCIAMACHY, these values refer to September–March. For these months and the addressed latitudinal range (43.93–48.09°N), the emission altitude of the SABER OH-B channel~~mean OH (3-1) emission altitude~~ presented in our fig. 2 (a) (thick line) reaches 84.5–87.5 km and shows reasonable agreement with a mean value of ca. 86 km~~ with 86.0–86.5 km~~. In contrast to our analysis, von Savigny (2015) refers to the centroid altitude, while we show the altitude of maximum VER. These values differ, if the OH VER profile is asymmetric. Furthermore, remaining tidal effects due to different overpass times of both satellites and vertical shifts between the different Meinel-bands may also play a role. So, considering these possible sources of inconsistencies, the agreement is even quite good.

As stated by Shepherd et al. (2006), the OH excitation mechanism is driven by atomic oxygen which is produced at higher altitudes. All processes which lead to vertical transport of atomic oxygen rich or poor air from above or below influence the OH production: when atomic oxygen rich air is brought down, the VER increases but the peak emission height decreases and vice versa. This relationship can be used for inferring the OH*-height from ground-based measurements alone (Liu and Shepherd, 2006; Mulligan et al., 2009). Liu and Shepherd (2006) show that the OH VER profiles are also broadened when the OH VER peak descends. This fits qualitatively to the yearly development of the FWHM and OH*-height (see fig. 2 (a) and (b)).

The latter seems to descend between 2002 and 2015. If one calculates the mean error of the yearly mean OH*-height which is the standard deviation (grey bars in fig. 2 (a)) divided by the square-root of the number of data points used per year (between 509 and 590, see section 2.2), the result reaches ca. 0.07 km (standard deviation of 1.5 km divided by $\sqrt{509}$). In fig. 2 (a), the OH*-height descends ca. 0.25 km in 14 years (ca. 0.02 km/a) which is significant within the error bars. This value lies in the same range as the ones derived by Bremer and Peters (2008) for low-frequency reflection heights (ca. 80–83 km) and by Teiser and von Savigny (2017) for the OH(3-1) centroid altitude based on SCIAMACHY measurements. Unfortunately, the SCIAMACHY results refer to latitudes between 5°S and 30°N, higher northern latitudes are not covered. ~~The authors~~Bremer and Peters (2008) investigated the annual means of the low-frequency reflection heights ~~of this parameter~~ measured at a constant solar angle with mid-point of the transmission path at 50.71° N and 6.61° E between 1959 and 2006. After elimination of the solar- and geomagnetically-induced signal, the authors deduce a trend of -0.032 km/~~a~~year. For the development of the OH*-equivalent BV frequency, this is currently not of importance: at least between 2007 and 2015, the OH*-equivalent BV frequency stayed constant (fig. 1 (c)). For the integration of a possible long-term development, it is therefore too early. However, it shows that this question needs to be revisited in a couple of years.

Formatiert: Nicht Hervorheben

Formatiert: Nicht Hervorheben

4 Summary and outlook

We investigate the OH*-layer height, FWHM, and OH*-equivalent BV frequency based on 14 years of TIMED-SABER data for 43.93–48.09°N and 5.71–12.95°E.

Their annual means reach ca. 86.5 km, 7.5 km, and 2.35×10^{-2} s^{-1} and are nearly stable during ~~14 years~~2002–2015. The characteristic intra-annual variations of the parameters lead to standard deviations of approximately 2% for the OH*-layer height, 10% for the OH*-equivalent BV frequency, and 20–30% for the FWHM.

Since the intra-annual variability dominates the inter-annual one by far, we can provide an analytic description for the mean OH*-equivalent BV frequency which is identical for every year. The superposition of an annual, semi-annual and ter-annual oscillation explains ca. 74% of the data variability. Ca. 85% or 98% of the data are located in a ±5%- or ±10%-interval around the mean curve.

Similar investigations are planned for other NDMC stations in order to facilitate the estimation of the nightly mean density of wave potential energy independent of co-located measurements which deliver vertical temperature profiles.

Acknowledgement

The work of Sabine Wüst was funded by the Bavarian State Ministry for the Environment and Consumer Protection (VAO-project LUDWIG, project number TUS01 UFS-67093).

References

Andrews, D. G.: An introduction to atmospheric physics, Cambridge University Press, 2000.

Baker, D. J., and Stair Jr., A. T.: Rocket measurements of the altitude distributions of the hydroxyl airglow, Phys. Scr., 37, 611–622, 1988.

Bills, R. E., and Gardner, C. S.: Lidar observations of the mesopause region temperature structure at Urbana, J. Geophys. Res., 98, 1011–1021, doi: http://dx.doi.org/10.1029/92JD02167, 1993.

Bittner, M., Offermann D., Bugaeva I. V., Kokin G.A., Koshelkov J. P., Krivolutsky A., Tarasenko D. A., Gil-Ojeda M., Hauchecorne A., Lübken F.-J., de la Morena B. A., Mourier, A., Nakane, H., Oyama, K. I., Schmidlin, F. J., Soule, I., Thomas, L., and Tsuda, T.: Long period/large scale oscillations of temperature during the DYANA campaign, J. Atmos. Terr. Phys., 56, 1675–1700, 1994.

Bremer, J., and Peters, D.: Influence of stratospheric ozone changes on long-term trends in the meso- and lower thermosphere, J. Atmos. Sol.-Terr. Phys., 70, 1473–1481, 2008.

Committee on Space Research; NASA National Space Science Data Center: COSPAR International Reference Atmosphere (CIRA-86): Global Climatology of Atmospheric Parameters, NCAS British Atmospheric Data Centre, 7th March 2017. http://catalogue.ceda.ac.uk/uuid/4996e5b2f53ce0b1f2072adadaeda262, 2006.

Hannawald, P., Schmidt, C., Wüst, S., and Bittner, M.: A fast SWIR imager for observations of transient features in OH airglow, Atmos. Meas. Tech. 9, 1461–1472, doi: 10.5194/amt-9-1461-2016, 2016.

Kramer, R., Wüst, S., Schmidt, C., and Bittner, M.: Gravity wave characteristics in the middle atmosphere during the CESAR campaign at Palma de Mallorca in 2011/2012: Impact of extratropical cyclones and cold fronts, J. Atmos. Sol.-Terr. Phys. 128, 8–23, doi: 10.1016/j.jastp.2015.03.001, 2015.

Garcia, F. J., Taylor, M. J., and Kelley, M. C.: Two-dimensional spectral analysis of mesospheric airglow image data, Appl. Opt., 36, 7374–7358, 1997.

Good, R. E.: Determination of atomic oxygen density from rocket borne measurement of hydroxyl airglow, Planetary Space Science, 24, 389–395, 1976.

Liu, G., and Shepherd, G. G.: An empirical model for the altitude of the OH nightglow emission, Geophys. Res. Lett., 33, L09805, doi: 10.1029/2005GL025297, 2006.

Lu, X., Liu, A. Z., Swenson, G. R., Li, T., Leblanc, T., and McDermid, I. S.: Gravity wave propagation and dissipation from the stratosphere to the lower thermosphere, J. Geophys. Res., 114, D11101, doi: 10.1029/2008JD010112, 2009.

Lu, X., Chu, X., Fong, W., Chen, C., Yu, Z., Roberts, B. R., and McDonald, A. J.: Vertical evolution of potential energy density and vertical wave number spectrum of Antarctic gravity waves from 35 to 105 km at McMurdo (77.8°S, 166.7°E), J. Geophys. Res. Atmos., 120, 2719–2737, doi: 10.1002/2014JD022751, 2015.

López-Puertas, M., Garcia-Comas, M., Funke, B., Picard, R. H., Winick, J. R., Wintersteiner, P. P., Mlynczak, M. G., Mertens, C. J., Russell III, J. M., and Gordley, L. L.: Evidence for an OH (v) excitation mechanism of CO_2 4.3 μm

nighttime emission from SABER/TIMED measurements, J. Geophys. Res., 109, D09307, doi: 10.1029/2003JD004383, 2004.

~~Garcia, F. J., Taylor, M. J., and Kelley, M. C.: Two-dimensional spectral analysis of mesospheric airglow image data, Appl. Opt., 36, 7374–7358, 1997.~~

~~Good, R.E.: Determination of atomic oxygen density from rocket borne measurement of hydroxyl airglow. Planetary Space Science, 24, 389–395, 1976.~~

Mertens, C. J., Schmidlin, F. J., Goldberg, R. A., Remsberg, E. E., Pesnell, W. D., Russell III, J. M., Mlynczak, M. G., López-Puertas, M., Wintersteiner, P. P., Picard, R. H., Winick, J. R., and Gordley, L. L.: SABER observations of mesospheric temperatures and comparisons with falling sphere measurements taken during the 2002 summer MaCWAVE campaign, Geophys. Res. Lett., 31, L03105, doi: 10.1029/2003GL018605, 2004.

Mertens, C. J., Fernandez, J. R., Xu, X., Evans, D. S., Mlynczak, M. G., and Russell III, J. M.: A new source of auroral infrared emission observed by TIMED/SABER, Geophys. Res. Lett. 35, 17–20, 2008.

Mlynczak, M. G.: Energetics of the mesosphere and lower thermosphere and the SABER experiment, Advances Space Res. 20, 1177–1183, doi: 10.1016/S0273-1177(97)00769-2, 1997.

Mulligan, F. J., Dyrland, M. E., Sigernes, F., and Deehr, C. S.: Inferring hydroxyl layer peak heights from ground-based measurements of OH (6-2) band integrated emission rate at Longyearbyen (78°N, 16°E), Ann. Geophys. 27, 4197–4205, doi: 10.5194/angeo-27-4197-2009, 2009.

Mzé, N., Hauchecorne, A., Keckhut, P., and Thétis, M.: Vertical distribution of gravity wave potential energy from long-term Rayleigh lidar data at a northern middle latitude site, J. Geophys. Res. 119, 12,069–12,083, doi: 10.1002/2014JD022035, 2014.

Noll, S., Kausch, W., Kimeswenger, S., Unterguggenberger, S., and Jones, A. M.: Comparison of VLT/X-shooter OH and O_2 rotational temperatures with consideration of TIMED/SABER emission and temperature profiles, Atmos. Chem. Phys. 16, 5021–5042, doi: 10.5194/acp-16-5021-2016, 2016.

Pautet, P.-D., Taylor, M., Pendleton, W., Zhao, Y., Yuan, T., Esplin, R., and McLain, D.: Advanced mesospheric temperature mapper for high-latitude airglow studies, Appl. Opt. 53, 5934–5943, 2014.

Placke, M., Hoffmann, P., Gerding, M., Becker, E., and Rapp, M.: Testing linear gravity wave theory with simultaneous wind and temperature data from the mesosphere, ~~J. Atmos. Sol. Terr. Phys.~~ J. Atmos. Sol.-Terr. Phys. 93, 57–69, doi: 10.1016/j.jastp.2012.11.012, 2013.

Rauthe, M., Gerding, M., and Lübken, F.-J.: Seasonal changes in gravity wave activity measured by lidars at mid-latitudes, J. Atmos. Chem. Phys. 8, 13741–13773, doi: 10.5194/acp-8-6775-2008, 2008.

Remsberg, E. E., Marshall, B. T., Garcia-Comas, M., Krueger, D., Lingenfelser, G. S., Martin-Torres, J., Mlynczak, M. G., Russell III, J. M., Smith, A. K., Zhao, Y., Brown, C., Gordley, L. L., Lopez-Gonzalez, M. J., Lopez-Puertas, M., She, C.-Y., Taylor, M. J., and Thompson, R. E.: Assessment of the quality of the Version 1.07 temperature versus pressure

profiles of the middle atmosphere from TIMED/SABER, J. Geophys. Res., 113, D17101, doi: 10.1029/2008JD010013, 2008.

Russell III, J. M., Mlynczak, M. G., Gordley, L. L., Tansock Jr., J. J., and Esplin, R. W.: Overview of the SABER experiment and preliminary calibration results, Proc. SPIE 3756, Optical Spectroscopic Tech. Instrum. Atmos. Space Res. III, 277–288, doi: 10.1117/12.366382, 1999.

Sedlak, R., Hannawald, P., Schmidt, C., Wüst, S., and Bittner, M.: High resolution observations of small scale gravity waves and turbulence features in the OH airglow layer, Atmos. Meas. Tech., 9, 5955–5963, doi: 10.5194/amt-2016-292, 2016.

She, C. Y., Yu, J. R., Huang, J. W., Nagasawa, C., and Gardner, C. S.: Na temperature lidar measurements of gravity wave perturbations of wind, density and temperature in the mesopause region, Geophys. Res. Lett., 18, 1329–1331, doi: 10.1029/91GL01517, 1991.

Shepherd, G. G., Cho, Y.-M., Liu, G., Shepherd, M. G., and Roble, R. G.: Airglow variability in the context of the global mesospheric circulation, J. Atmos. Sol. Terr. Phys. J. Atmos. Sol.-Terr. Phys., 68, 2000–2011, doi: 10.1016/j.jastp.2006.06.006, 2006.

Teiser G., and von Savigny, C.: Variability of OH(3-1) and OH(6-2) emission altitude and volume emission rate from 2003 to 2011, J. Atmos. Sol.-Terr. Phys., 161, 28–42, 2017.

Tsuda, T., Nishida, M., Rocken, C. H., and Ware, R. H.: A global morphology of gravity wave activity in the stratosphere revealed by the GPS occultation data (GPS/MET), J. Geophys. Res. 105, 7257–7273, doi: 10.1029/1999JD901005, 2000.

von Savigny, C.: Variability of OH (3-1) emission altitude from 2003 to 2011: Long-term stability and universality of the emission rate-altitude relationship, J. Atmos. Sol. Terr. Phys. J. Atmos. Sol.-Terr. Phys., 127, 120–128, doi: 10.1016/j.jastp.2015.02.001, 2015.

von Savigny, C., McDade, I. C., Eichmann, K. U., and Burrows, J. P.: On the dependence of the OH* Meinel emission altitude on vibrational level: SCIAMACHY observations and model simulations, Atmos. Chem. Phys., 12, 8813–8828, doi: 10.5194/acp-12-8813-2012, 2012.

von Zahn, U., Fricke, K. H., Gerndt, R., and Blix, T.: Mesospheric temperatures and the OH layer height as derived from ground-based lidar and OH* spectrometry, J. Atmos. Terr. Phys., 49, 863–869, 1987.

Wachter, P., Schmidt, C., Wüst, S., and Bittner, M.: Spatial gravity wave characteristics obtained from multiple OH (3-1) airglow temperature time series, J. Atmos. Sol.-Terr. Phys. 135, 192–201, doi: 10.1016/j.jastp.2015.11.008, 2015

Wendt, V., Wüst, S., Mlynczak, M. G., Russell III, J. M., Yee, J.-H., and Bittner, M.: Impact of atmospheric variability on validation of satellite-based temperature measurements, J. Atmos. Sol.-Terr. Phys. 102, 252–260, doi: 10.1016/j.jastp.2013.05.022, 2013.

Formatiert: Nicht Hervorheben

Formatiert: Nicht Hervorheben

Wüst, S., and Bittner, M.: Non-linear resonant wave-wave interaction (triad): Case studies based on rocket data and first application to satellite data~~.~~ ~~J. Atmos. Sol. Terr. Phys.~~ J. Atmos. Sol.-Terr. Phys., 68, 959–976, doi: 10.1016/j.jastp.2005.11.011, 2006.

Wüst, S., Wendt, V., Schmidt, C., Lichtenstern, S., Bittner, M., Yee, J.-H., Mlynczak, M. G., and Russell III, J. M.: Derivation of gravity wave potential energy density from NDMC measurements, ~~J. Atmos. Sol. Terr. Phys.~~ J. Atmos. Sol.-Terr. Phys., 138, 32–46, doi: 10.1016/j.jastp.2015.12.003, 2016.

Wüst, S., Schmidt, C., Bittner, M., Price, C., Silber, I., Yee, J.-H., Mlynczak, M. G. and Russell III, J. M.: First ground-based observations of mesopause temperatures above the Eastern-Mediterranean Part II: OH*-climatology and gravity wave activity, ~~J. Atmos. Sol. Terr. Phys.~~ J. Atmos. Sol.-Terr. Phys., 155, 104–111, doi: 10.1016/j.jastp.2017.01.003, 2017.

Zhang, S. P., and Shepherd, G.: The influence of the diurnal tide on the O(1S) and OH emission rates observed by WINDII on UARS, Geophys. Res. Let., 26, 529–532, 1999.

Formatiert: Block, Einzug: Links: 0 cm, Hängend: 0,5 cm, Zeilenabstand: 1,5 Zeilen

	~~1st oscillation~~"annual" oscillation	~~2nd oscillation~~"semi-annual" oscillation	~~3rd oscillation~~"ter-annual" oscillation
Period T [d]	364.7	182.4	121.3
Amplitude A [10^{-2} s^{-1}]	0.19	0.07	0.05
Phase φ [rad]	1.70	-1.69	2.36

Table 1: Period, amplitude and phase of the three oscillations which explain the variability of the daily OH*-equivalent BV frequency values (averaged over all years) best. They oscillate around a constant value of 2.32 ~~×~~ 10^{-2} s^{-1}. The OH*-equivalent BV frequency [s^{-1}] can be estimated by $2.32 \times 10^{-2} + \sum_{i=1}^{3} A_i \sin\left(\frac{2\pi}{T_i} \cdot DoY - \varphi_i\right)$. Due to leap years, the total amount of days for one year is set to 366, that means 1st March is DoY 61 for every year.

(a)

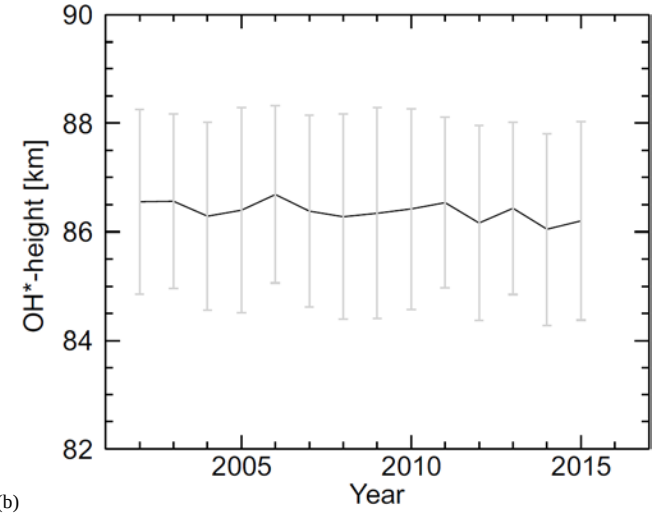
90
88
86
84
82
OH*-height [km]
2005
2010
2015
Year

(b)

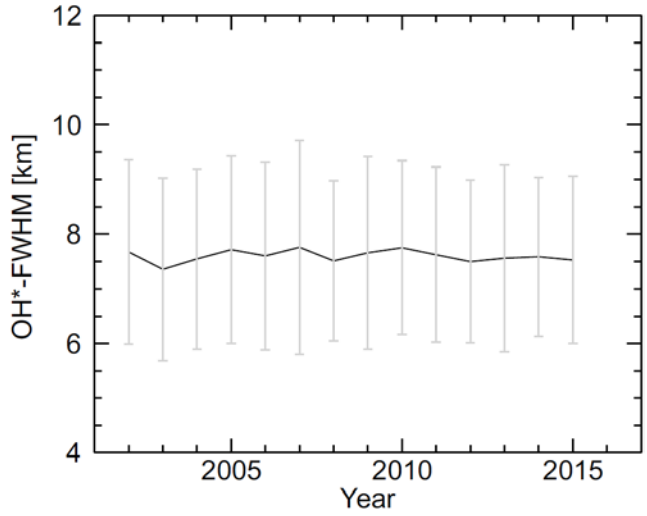
12
10
8
6
4
OH*-FWHM [km]
2005
2010
2015
Year

(c)

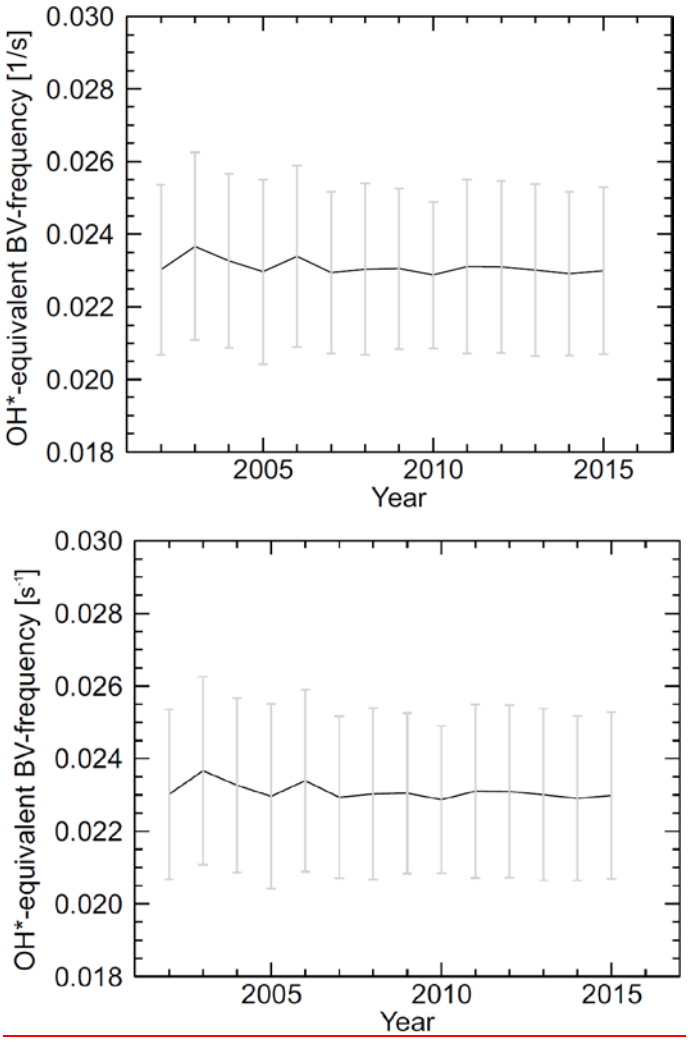

Figure 1: The yearly means of the height of the maximal OH-VER (denoted as OH*-height, see part a), the FWHM (part b), and the OH*-equivalent BV frequency (part c) are nearly constant from 2002 to 2015 (black curve) but show ~~a~~ comparatively large standard deviations (grey bars) for each year.

(a)

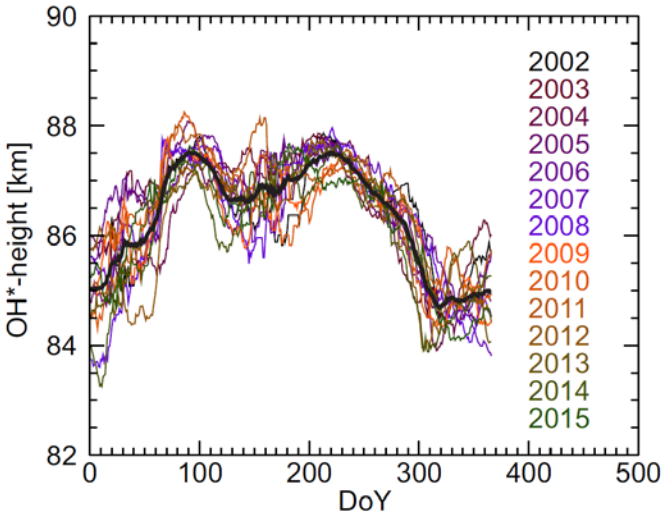
OH*-height [km]
DoY
2002
2003
2004
2005
2006
2007
2008
2009
2010
2011
2012
2013
2014
2015

(b)

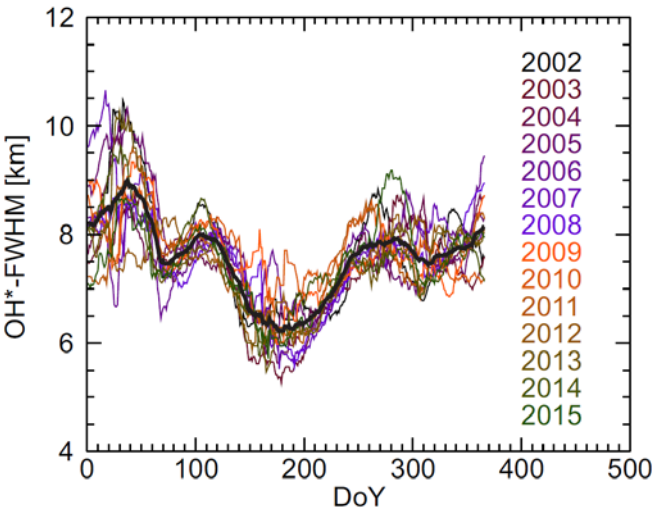
OH*-FWHM [km]
DoY
2002
2003
2004
2005
2006
2007
2008
2009
2010
2011
2012
2013
2014
2015

(c)

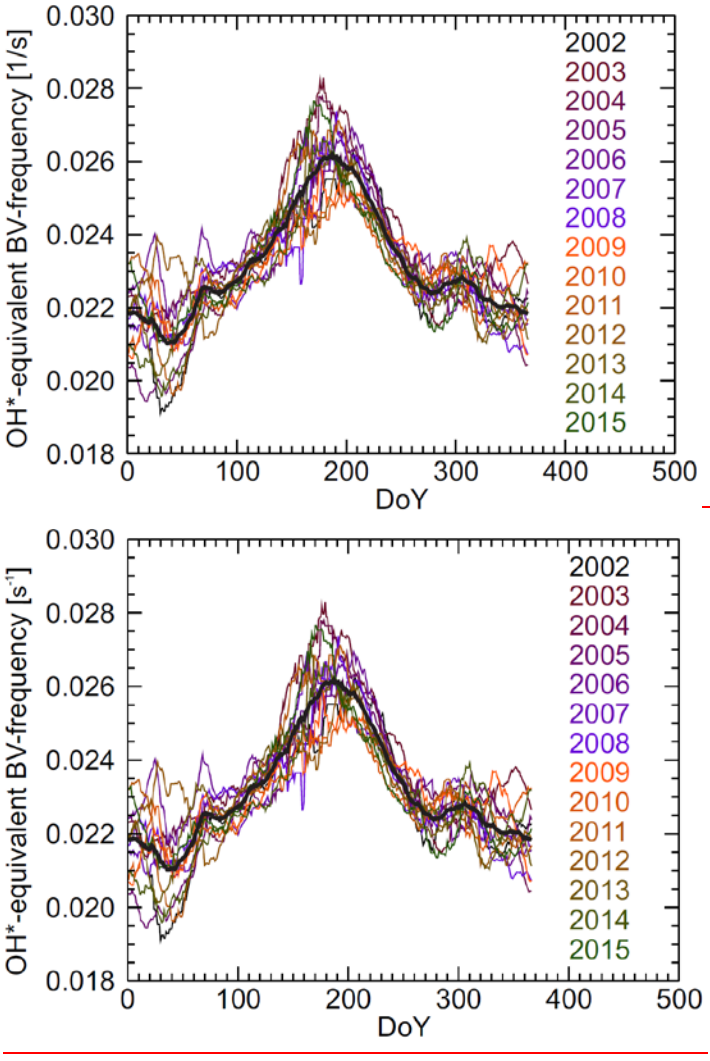

Figure 2: OH*-height (part a), FWHM (part b), and OH*-equivalent BV frequency (part c) show characteristic variations during the year (coloured lines: 30-point running means of the daily mean values with mirrored edge points for the beginning of 2002 and the end of 2015). The values of the individual years deviate most from the mean over all years (black line) during winter and especially at the beginning of the year. This might be due to enhanced atmospheric dynamics which is for example represented by stratospheric warming events and its effects on the mesopause.

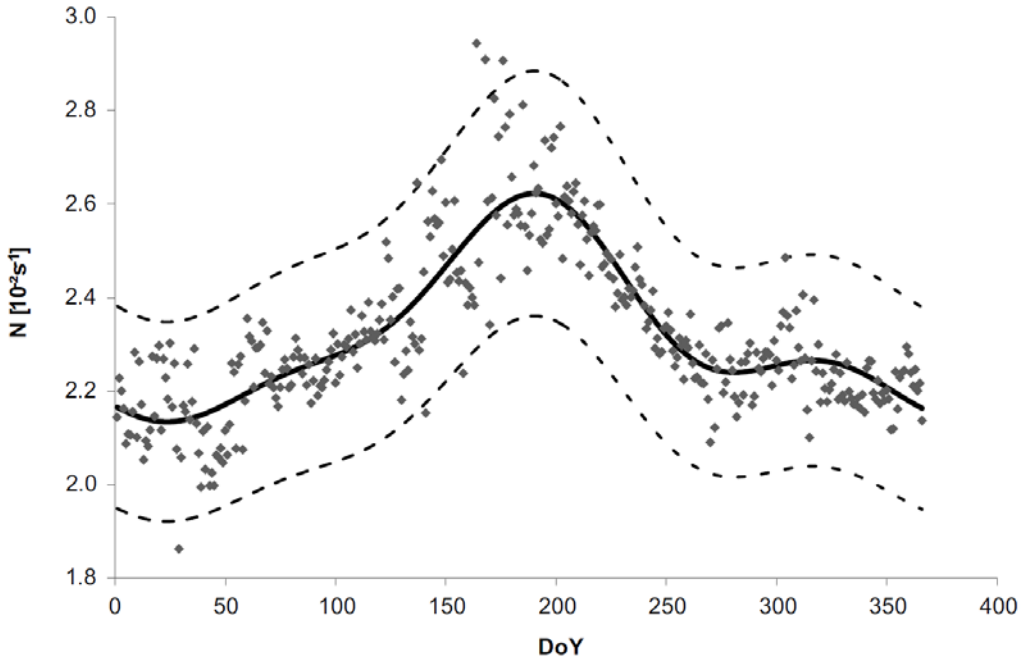

Figure 3: The superposition of the annual, semi-, and ter-annual oscillation (solid line) explains ca. 74 % of the variability of the daily OH*-equivalent BV frequency values averaged over all years (diamonds). 97.8% of the data are located in a ±10%-interval (dashed lines) around the curve.

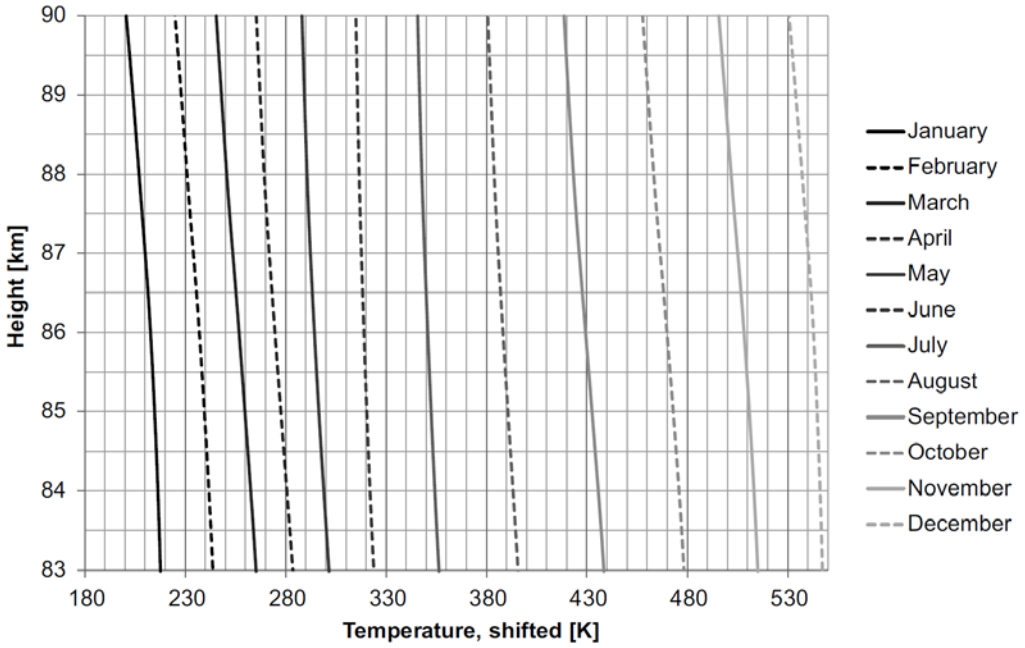

Figure 4: The temperature gradient based on CIRA-86 data for 45°N between 83 and 90 km height is negative during the whole year. The steepest gradient is reached in March and September (ca. 20 K / 7 km), it differs least from zero in summer (June–July, ca. 10 K / 7 km). The temperature values are ~~shifted~~ offset by +30 K per month for all months except January.